Fracture Mechanics of Concrete and Concrete Structures - Assessment, Durability, Monitoring and Retrofitting of Concrete Structures- B. H. Oh, et al. (eds)

Effect of hogging moment on FRP debonding from the substrate of concrete beams

J.L. Pan
Key Laboratory of Concrete and Pre-stressed Concrete structures of Ministry of Education, Southeast University, China

Trevor C.F. Chung, Christopher K.Y. Leung
Hong Kong Univiversity of Science and Technology, Hong Kong

ABSTRACT: In recent two decades, the bonding of fiber reinforced polymer (FRP) on the tensile side of concrete members has been accepted as an effective and efficient method for strengthening and retrofitting concrete structures. In the present study, to investigate the failure behavior of the FRP strengthened concrete beams under practical conditions, the experimental tests different from the three-point or four-point bending tests are performed. To simulate a continuously supported concrete member, hogging moments are applied on the two ends of a beam specimen to achieve compression zones near the supports. The experimental parameters include the hogging-to-sagging moment ratio, the distance between the plate end and the support, FRP thickness and so on. According to the test results, with end zones of the FRP plate anchored within the compression zone, the longitudinal compression around the plate end can lead to a transition of failure mode from plate end failure to crack-induced debonding, associating with a corresponding enhancement of the moment capacity. For the beams failed in the mode of intermediate crack induced debonding, increasing the distance between the plate end and the support caused decrease of the ultimate debonding moment. For the beams with different hogging-to-sagging moment ratios, increasing the plate thickness may result in change of the failure mode or increase of the ultimate failure moment.
KEY WORDS: FRP; Concrete beams; Hogging-to-sagging moment ratio; Failure behaviour.

1 INTRODUCTION

In the last two decades, the external bonding of fiber reinforced polymer (FRP) has become increasingly popular for strengthening and retrofitting of concrete structures due to superior properties of FRP composites, such as high strength-to-weight ratio, high corrosion resistance, ease of application and good durability (Meier 1997). This new strengthening technique involves bonding FRP plates or sheets on the tension side of a concrete beam, and has been proved to be effective in increasing both the stiffness and the load carrying capacity (Ritchie et al. 1991, Saadatmanesh & Ehsani 1991, Meier et al. 1992). For the strengthened concrete members, various failure modes have been observed in existing experimental investigations (Meier 1995, Arduini et al. 1997, Buyukozturk et al. 1998). These failure modes can be categorized into six types under three distinct failure mechanisms, which are (1) flexural failure, including FRP rupture or concrete crushing in the compression zone (with or without yielding of tensile steel), (2) shear failure and (3) local failure, including concrete cover separation, plate end interfacial debonding and crack-induced debonding. When the failure is due to flexural failure (i.e. concrete crushing or FRP rupture), the failure load of the strengthened member can be simply calculated based on the conventional section analysis for reinforced concrete (RC) beams. For this failure mode, the amount of FRP should be chosen carefully to ensure yielding of tensile steel and sufficient warning before the ultimate failure can be obtained. However, it is more common that the failure of the strengthened member is found to occur accompanied with premature debonding of the FRP plate from the concrete beam. With different combination of parameters, debonding may occur from the plate end or the bottom of a major crack in the span. Up to now, a number of theoretical models have been proposed for predicting the debonding failure of the FRP plate from concrete beams.

Figure 1 shows a FRP strengthened concrete beam with the failure mode of FRP debonding from a major flexural or shear/flexural crack in the span. For a major flexural crack in the beam, there is no vertical displacement between the two sides of the crack. Debonding is considered to be caused by high shear stresses along the concrete-to-FRP interface

around the bottom of the crack. With increasing loading, the interfacial debonding will propagate towards the free end of the FRP plate, leading to ultimate debonding failure. The inter- mediate flexural crack induced debonding is often regarded as mode II (shear mode) debonding failure (Leung & Tung 2006), which can be modeled by a pull-off test. Various bond slip models have been proposed for predicting the debonding behavior and the bond strength between the FRP plate and concrete (Taljsten 1996, Bizindavyi & Neale 1999, Chen & Teng 2001, Leung & Tung 2006, Wang 2006). With the maximum FRP stress/strain from the above mentioned models, the ultimate load capacity of the beam, which fails by FRP debonding from a major flexural crack, can approximately be calculated by sectional analysis for RC beams. However, for the strengthened concrete beams, debonding failure may also initiate from the bottom of a flexural/shear crack in the span (Fig. 1). For the flexural shear crack, there are both horizontal and vertical displacements between the two sides of the crack. With opening of the flexural/shear crack, high peeling and shear stresses are induced at the interface between the FRP plate and concrete, leading to premature debonding of the FRP plate from the substrate of the concrete beam. Teng et al. (2003) considered that the peeling effect caused by the flexural/shear crack was a secondary factor governing the intermediate crack induced debonding. Recently, some experimental and theoretical investigations have focused on debonding failure caused by a flexural/shear crack. Niu et al (2006) described the debonding behavior initiated from a diagonal crack through finite element analysis. Wang (2007) developed a cohesive zone model for mixed mode debonding of the FRP plate from the concrete substrate. Based on the experimental results, Pan & Leung (2007) proposed a four-parameter model for studying FRP debondong under both pulling and peeling effects. The vertical displacement between the two sides of the flexural/shear crack makes debonding much easier to initiate than mode II debonding. Both experimental and numerical results show that the peeling effect on the debonding decreases with the propagation of the interfacial crack, and the mixed mode debonding can be modeled as Mode II debonding when the size of the debonded zone is long enough.

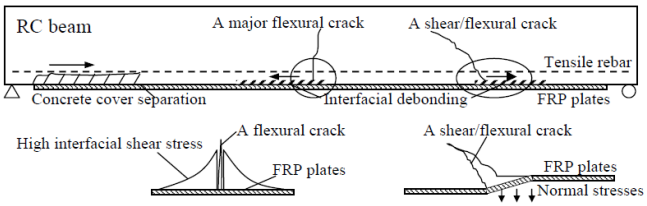

Figure 1. Debonding failure in FRP strengthened concrete beam.

Apart from intermediate crack induced debonding, debonding failure may also initiate from the end of the FRP plate (Fig. 1). This debonding failure usually involves separation of the concrete cover from the rest of the member at the plate end (Sharif et al. 1994, Nguyen et al. 2001, Gao et al. 2005). The plate end debonding failure (or concrete cover separation) is initiated from a crack near the plate end, due to high interfacial shear and normal stresses caused by the abrupt termination of the plate (Saadatmanesh & Malek 1998). For this debonding failure, a number of theoretical models have been developed for predicting the failure load of the strengthened beams (Smith & Teng 2002, Ahmed et al. 2001, Malek et al. 1998, Raoof 2000, Gao et al. 2005). These models can be classified into three categories, namely (i) interfacial stress based models (Ziraba et al. 1994), (ii) shear capacity based models (Oehlers 1992, Jansze 1997), and (iii) concrete tooth models (Raoof & Zhang 1997, Raoof & Hassanen 2000).

In most existing experiments, the concrete beams bonded with FRP plates are commonly loaded in three or four-point bending, resulting in tensile stresses all along the FRP plate. However, in real structures, for the continuous reinforced concrete beam strengthened by FRP plates, FRP plates may be subjected to compression in the regions of negative moment and subjected to tension in the regions of positive moment. Experimental investigations regarding the bonded plate under longitudinal compression are very limited. As stated by CEB-fib (2001), external bonded FRP plates may fail by local buckling at relatively low compressive stress levels, but no rigorous investigations have been provided to verify this argument. In the present investigation, a number of FRP strengthened concrete beams are tested to study the effect of hogging moments on the interaction between the FRP plate and the concrete. With different hogging-to-sagging moment ratios, the influence of compression at plate ends can be investigated. Plate thickness is another experimental parameter as it can affect the shear transferring behavior, the ultimate capacity and the failure mode of the specimen.

2 EXPERIMENTAL PROGRAM

In the present experiments, seventeen FRP strengthened concrete beams are tested with different hogging-to-sagging moment ratios, different distance between the plate end and the support, and different FRP thicknesses (Fig. 2). To generate the hogging moments for the specimens, the beams are cantilevered at both ends and two loading points locate outside the supported span. For ease of result presentation, the notation of the specimens is described as follows. For example, for the specimen C10-M025-L6, “C” refers to tests with the plate ends terminated within the compression zone, and the number that follows “C” denotes the specimen number. The second part of the notation specifies the hogging-to-sagging moment

ratio of the specimen. For instance, "M025" indicates that the specimen is loaded with a ratio of 0.25 between the maximum hogging and sagging moments. The last part gives the layers of FRP sheets which are bonded on the specimen and the letter "t" denotes tapered FRP plate are employed to decrease the stress concentrations at the plate end.

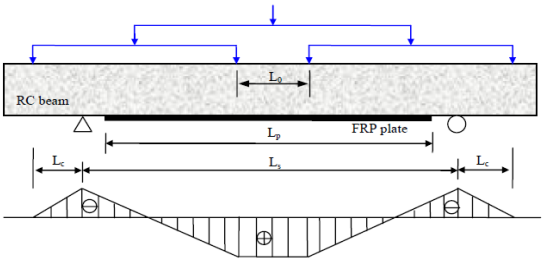

Figure 2. Load configuration for the beams with different sagging-to-hogging moment ratios.

2.1 *Material properties*

The concrete used for casting the beams was ordered from a commercial concrete supplier to ensure consistent properties for all the specimens. After curing in the standard curing condition for 28 days, the cylinder compressive strength was tested to be 59 MPa. For all specimens, two high yield steel rods of 10 mm in diameter, with yielding strength of 550 MPa and Young's Modulus of 202 GPa, were used as the tensile reinforcement. For compression steel reinforcement, two mild steel bars with diameter of 8 mm were placed at a depth of 36 mm from the top surface of concrete beams. To avoid shear failure of the beam specimens, a number of mild steel stirrups (with diameter of 12 mm) are uniformly placed along the span with a center-to-center spacing of 80 mm along the span. Above each support, two ribbed bars of 20 mm diameter are provided to resist the hogging moment around the support zone.

For strengthening the concrete beams, unidirectional carbon fiber reinforced polymer (CFRP) was applied through the wet lay-up process. The material properties of FRP composites are provided by the producer. The nominal thickness for each ply is 0.11 mm. The tensile strength along the fiber direction is 4200 MPa and the Young's modulus is 235 GPa. For all beam specimens, the bonded plate has the same width as the concrete beams, which is 150 mm. The CFRP is a brittle material which shows linearly elastic stress-strain behavior up to final brittle rupture under tension. Two types of epoxy resins, including epoxy primer and epoxy resin, were used to bond FRP sheets on the concrete substrates. To perform the bonding, the hardener was mixed thoroughly into the resin with a ratio of 1:3 by weight. According to the product specification, the tensile modulus, shear modulus and Poisson's ratio of the epoxy resin were tested to be 3.5GPa, 1.28GPa and 0.37, respectively. The mean thickness of the adhesive is estimated to be about 2 mm.

2.2 *Specimen preparation*

In the experiments, each beam specimen is 150 mm in width and 200 mm in depth, and is reinforced with two ribbed bars of 10 mm diameter at an effective depth of 163 mm. Inside the member, 12 mm diameter stirrups made of mild steel spaced at 80 mm were employed to avoid shear failure. For all the specimens, two 20 mm diameter ribbed tension bars are provided to resist the hogging moment above the supports. In order to generate longitudinal compression around the plate ends, cantilevers are left on the two sides of the supported span and loading is applied on the cantilever with the help of a wiffle-tree system in Figure 2. Different levels of hogging moment can be adjusted by moving the loading points to different position of the

Table 1. Dimensional information and test results for the tested beams.

Specimen	FRP layers	L_e (mm)	L_s (mm)	L_c (mm)	M_H:M_S	M_{PE}:M_S	Shear Span (mm)	Max. FRP Strain (10^{-6})	Max. moment (kNm)	Failure mode
C1-M0-12	2	100	2200	0	0	0.10	1000	10753	29.6	IC
C2-M033-12	2	100	2200	250	-0.33	-0.20	750	9973	28.4	IC
C3-M1-12	2	100	2200	500	-1	-0.80	500	13192	33.4	IC
C4-M0-16	6	200	2200	0	0	0.20	1000	5989	40.8	IC
C5-M043-16	6	200	2200	300	-0.43	-0.14	700	6508	43.2	IC
C6-M067-16	6	200	2200	400	-0.67	-0.33	600	6484	43.1	IC
C7-M1-16	6	200	2200	500	-1	-0.60	500	5624	39.1	IC
C8-M089-16	6	400	1900	400	-0.89	0.00	450	4196	35.6	IC
C9-M089-16	6	300	1900	400	-0.89	-0.22	450	5175	42.8	IC
C10-M089-16	6	200	1900	400	-0.89	-0.44	450	5215	43.1	IC
C11-M089-16t	6	100,200,300	1900	400	-0.89	-0.67	450	4689	41.9	IC
C12-M089-16t	6	100,200	1900	300	-0.56	-0.67	550	5122	41.8	IC
C13-M0-16	6	100	1900	0	0.00	0.125	800	4655	33.8	PE
C14-M014-16	6	100	1900	100	-0.14	0.00	700	5492	44.1	IC
C15-M033-16	6	100	1900	200	-0.33	-0.17	600	5326	42.5	IC
C16-M06-16	6	100	1900	300	-0.60	-0.40	500	4432	40.3	IC
C17-M1-16	6	100	1900	400	-1.00	-0.75	400	4307	37.9	IC

span outside the supports. The detailed dimensional information about the beam specimens is shown in Table 1. The hogging-to-sagging moment ratio ranges from 0 to 1 in the tests.

After the concrete specimens were cured for 28 days, FRP sheets were applied to form the bonded plate. Before applying the FRP, the tensile surface of the concrete beam was roughened with a needle gun to expose the aggregate and cleaned by pressured air to remove the dust. Then, epoxy primer was applied to improve the bond between concrete and FRP sheets. After the primer hardened, FRP sheets were bonded to the tensile side of the concrete beam layer by layer until the required thickness was reached. For each beam specimen, the plate end was kept a certain distance from the nearer support. To ensure full hardening of the epoxy based FRP plate, the beam specimens were cured for another seven days before testing. The detailed information of the specimens is shown in Table 1.

2.3 *Testing and Instrumentation*

All tests were conducted on a hydraulic loading machine DARTEC 2500 with the maximum capacity of 2500 kN. In the tests, the specimens were loaded under stroke control with a loading rate of 0.01 mm/s. The force exerted by the machine was measured using a calibrated load cell and the stroke was measured with an internal Linear Variable Differential Transformer (LVDT). During the test, the collected data included the force applied by the testing machine, the displacement of the ram, the mid-span deflection of the beam measured by a LVDT and strains measured by six electrical resistance strain gauges along the FRP plate. Simultaneous data collection during testing was carried out with an automatic data logger.

3 TEST RESULTS AND DISCUSSIONS

3.1 *Failure characterization*

In the experiments, the beams with two plies of FRP all failed by intermediate crack induced debonding. Figure 3 depicts the moment responses of all the 2-ply beams. For specimens with low hogging moment, i.e. C1-M0-L2 and C2-M033-L2, the initial cracks occurred at about 6 kNm, and steel yielded at the moment of about 20 kNm. With further increasing load, initial debonding of the FRP plate from the bottom of an intermediate crack occurred, as shown in Figure 4. This brittle failure was accompanied by a sharp drop of external moment, and the residual moment was very close to the yielding moment of the beam before strengthening. For C2-M033-L2, instead of a sudden debonding, the interfacial crack stopped near the point where the sectional moment was zero, resulting in a partial drop of the moment (Fig. 4). From the figure, the behaviors of C1-M0-L2 and C2-M033-L2 are similar before debonding. The latter specimen has a slightly higher stiffness after the first set of cracks occurred. For the specimen with higher hogging moment (C3-M1-L2), it shows higher stiffness and its debonding moment increases by 12.8% compared to the other two specimens. However, in this case, the lowest deflection at debonding is obtained, indicating that the ductility of the specimen is decreased.

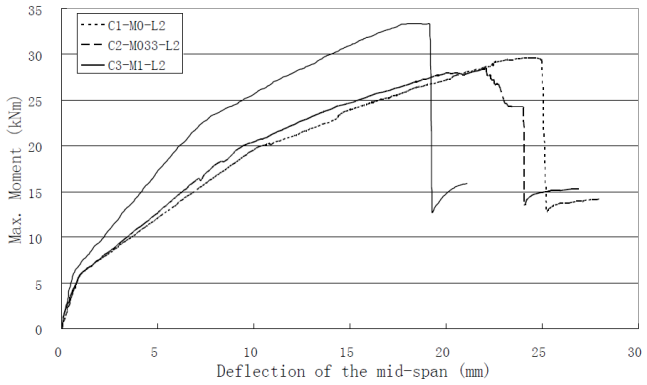

Figure 3. Moment-deflection curves for the specimens strengthened with 2 FRP layers.

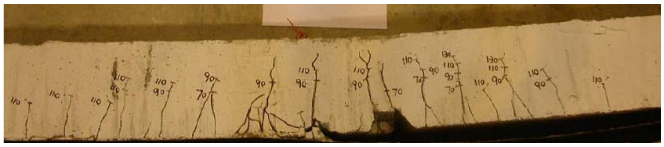
Figure 4. Final crack pattern for the beam C2-M033-L2.

With increasing the plate thickness, the debonding behavior was very different from the two-ply specimens. In the experiments, sixteen 6-ply beams were tested to investigate the failure mechanism of the strengthened beams. The experimental parameters include the hogging-to-sagging moment ratio (η), the distance between the plate end and the near support (L_e). According to the test results, with different combination of the experimental parameters, the strengthened beams may fail by plate end failure (concrete cover separation) or intermediate crack induced debonding. To clarify the failure characteristics of the two failure modes, the deflection-moment curves (Fig. 5) of two typical strengthened specimens (C13-M0-L6 and C5-M043-L6) will be employed to describe the debonding processes. For the specimen C13-M0-L6, there was no hogging moment was applied, the strengthened beam failed in the mode of concrete cover separation. When the applied moment was below 5.6 kNm, the strengthened beam was still in elastic stage, and there were no cracks along the span. With increasing external load, distributed flexural

and flexural/shear cracks started to occur along the span of the strengthened beam, resulting in a reduction of the stiffness. The displacement in the middle of the span increased more quickly with the external loading. When the moment reached about 22.3 kNm, a flexural-shear crack formed at or near the plate end. With further increase of the external loading, this crack tended to grow into the concrete compression zone, towards the direction of the nearer loading point. When the crack was arrested by the internal stirrups, a peeling crack developed at the level of the internal bars. The propagation of this crack was immediately followed by the peel-off of the concrete cover as shown in Figure 6.

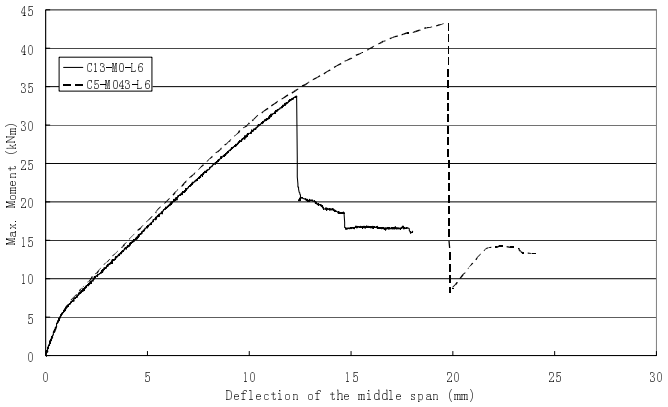

Figure 5. Moment-deflection curves for two typical specimens with 6 FRP layers.


Figure 6. Concrete cover separation for the beam C13-M0-L6.

For the specimen C5-M043-L6, the ratio between the hogging and sagging moment was 0.43, and this strengthened beam failed in the mode of intermediate crack induced debonding. When the applied moment at the middle span was smaller than 7 kNm, the strengthened beam was still in elastic stage and the deflection of the beam increased linearly with the external moment. With further loading, a set of cracks formed at the middle span with a sudden change of stiffness. The deflection of the beam still increased linearly with increasing moment until the yielding point of the tension reinforcement was reached. Initial debonding of the FRP plate occurred from the bottom of a major flexural crack at the middle span at about 35 kNm. With increasing moment, debonding of the FRP plate gradually propagates along the concrete- to-FRP interface until final failure. The final crack pattern of the strengthened beam is shown in Figure 7.


Figure 7. Intermediate crack induced debonding for the beam C5-M043-L6.

3.2 *Effect of hogging-to-sagging moment ratios*

For simply supported FRP strengthened concrete beams, the FRP plates were externally bonded on the bottom of the beam and totally located below the center line of the strengthened beam. Under external loading, the whole FRP plate is in tension, which may induce high peeling and shearing stresses at the FRP-to-concrete interface at the end of the FRP plate or at the bottom of flexural-shear cracks. However, for the continuous concrete beams, there is significant hogging moment for the sections near the support. The FRP plates terminated near the supports may be subjected to compression in the regions near the plate ends. In the present experiments, eleven strengthened beams were tested to investigate the effect of hogging-to-sagging moment ratio on the failure behavior of the strengthened beams. The eleven strengthened beams can be categorized into two series according to the size of the clear span. For the strengthened beams with the clear span of 2200 mm, they all failed in the mode of intermediate crack induced debonding for all hogging-to-sagging moment ratios. For this series, the beam with moderate hogging- to-sagging moment ratio had the highest ultimate moment (Fig. 8). Interestingly, the plate end of this beam just located at the location where the bending moment was zero, resulting in smallest stress concentrations at the plate end. For the beams with the clear span of 1900mm, the failure mode of the beams transferred from concrete cover separation to intermediate crack induced debonding with increasing the hogging-to-sagging moment ratio. However, for the beams with the same failure mode, i.e., intermediate crack induced debonding, the beam with moderate hogging-to-sagging moment ratio showed the highest ultimate moment as the foregoing series of beams, as shown in Figure 8. This phenomenon indicates that the ultimate moment is not only affected by the hogging- to-sagging moment ratio but also affected by the bending moment at the plate ends.

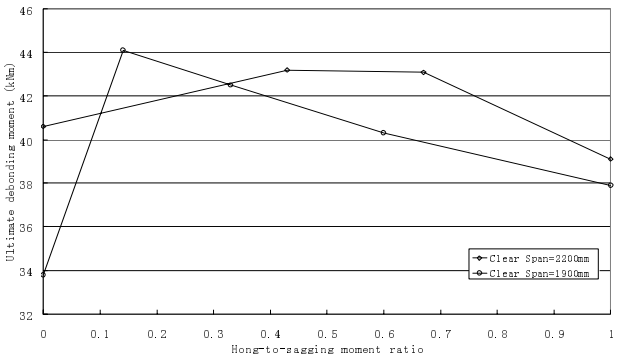

Figure 8. Relationship between the hogging-to-sagging moment ratio and ultimate debonding moment.

3.3 *Effect of distance between the plate end and the support*

In the experiments, five strengthened beams were tested to investigate the effect of the distance between the plate end and the support on debonding behavior under the presence of hogging moment near the supports. For these strengthened beams, the hogging-to-sagging moment ratio was set to be 1.0, except for the beam C12-M06-l6t, whose hogging- to-sagging moment ratio was 0.6. Moreover, the beams C12-M06-l6t and C11-M089-l6t were strengthened with tapered FRP plates. A stake of 100 mm was set for each two layers of FRP sheets for the beam C11-M1-l6t, and for each three layers of FRP sheets for the beam C12-M06-l6t. By varying the distance between the plate end and the support, various ratios between the plate end moment and the maximum sagging moment can be obtained. According to the test results, all beams failed in the mode of intermediate crack induced debonding. As shown in Figure 9, the ultimate debonding moment decreased with the distance between the plate end and the support. The ultimate debonding moment of the beam C8-M089-l6, which had the largest distance between the plate end and the support (Le=400mm), was 18% to 21.2% lower than that of the other beams. Also, for the beamC8-M089-l6, the maximum FRP strain was 10.5% to 19.5% lower than that of the other beams. The larger the distance between the plate end and the support, the shorter the region anchored in the compression zone. Therefore, the beam with larger Le will easily debond at a smaller external moment.

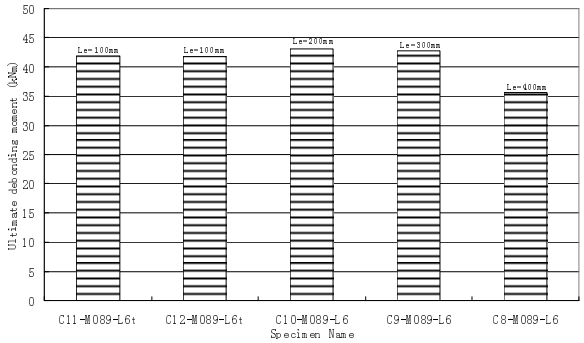

Figure 9. Relationship between Le and the ultimate debonding moment.

3.4 *Effect of the thickness of FRP plate*

In the present experiments, the strengthened beams with 2 and 6 FRP sheets were tested. According to the test results, for the beams without hogging moment at the supports, with increasing the thickness of the FRP plate, the failure mode changed from the IC debonding to concrete cover separation. For the beams with hogging moment at the support, increasing the thickness of the FRP plate may not cause change of the failure mode, but led to a significant increase of the ultimate debonding moment. For the beams C2-M033-l2 and C16-M033-l6, they both failed in the mode of IC debonding, but the ultimate debonding moment for the beam C15-M033-l6 was 49.6% higher than that of the beam C2-M033-l2. The same trend is found for the other beams.

4 CONCLUSIONS

In this paper, experimental investigations have been conducted to study the structural behavior of FRP strengthened RC beams under the presence of hogging moment near the supports. Based on the test results, for the strengthened beams, the ultimate debonding moment was governed by the parameters including the hogging-to-sagging moment ratio, the distance between the plate end and the support, the thickness of the FRP plate and so on. For the beams with the same FRP thickness and relative small distance between the plate end and the support, the failure mode can change from concrete cover separation to intermediate crack induced debonding with increasing the hogging-to-sagging moment ratio. In this case, moderate hogging-to-sagging moment ratio can result in the highest debonding moment for the beams failed in intermediate crack induced debonding. For the beams with the same hogging-to-sagging moment and the same FRP thickness, the ultimate debonding moment decreased with the distance between the plate end and the support. For the beams with the same hogging-to-sagging moment, increasing the plate thickness may cause the change of the failure mode from the IC debonding to concrete cover separation, or cause significant increase of the failure moment in the same failure mode in terms of the value of the hogging-to-sagging moment ratio.

ACKNOWLEDGMENT

Financial support of the work by the Hong Kong Research Grant Council under CERG UST6252/02E, by Natural Science Foundation of Jiangsu Province under BK2007567 and by the Research Fund for the

Dectoral Program of Higher Education under 20070286024 is gratefully acknowledged.

REFERENCE

Ahmed, O., Gemert, D.V., and Vadewalle, L. (2001), *Improved Model for Plate-End Shear of CFRP Strengthened RC Beams*, Cement and Concrete Composites, Vol. 23, pp. 3-19.

Arduini M., and Nanni A., "Behavior of precracked RC beams strengthened with carbon FRP sheets", *Journal of Composites for Construction,* vol. 1, no. 2, pp. 63-70, 1997.

Bizindavyi L. and Neale K.W. (1999). "Transfer length and Bond strengths for composites bonded to concrete." *Journal of composites for construction*, 3(4), 153-160.

Buyukozturk O. and Hearing B., "Failure behaviour of precracked concrete beams retrofitted with FRP", *Journal Composites for Construction*, vol. 3, pp. 38-144.1998.

Bo Gao, Jang-Kyo Kim, and Christopher K.Y. Leung. (2005). "Optimization of tapered end design for FRP strips bonded to RC beams", *Journal of composites science and Technology*, Vo.66, No.10, pp.1266-1273.

Chen J.F. and Teng J.G. (2001). "Anchorage strength models for FRP and steel plates attached to concrete", *Journal of Structural Engineering*, ASCE, 127(7), 784-791.

fib (2001), Externally Bonded FRP Reinforcement for RC Structures: Technical Report on the Design and Use of Externally Boded Fibre Reinforced Polymer Reinforcement (FRP EBR) for Reinforced Concrete Structures, International Federation for Structural Concrete (fib), Lausanne, Switzerland.

Jansze, W. (1997), Strengthening of Reinforced Concrete Members in Bending by Externally Bonded Steel Plates: Design for Beam Shear and Plate Anchorage, Delft University Press, The Netherlands.

Leung, C.K.Y. and Tung, W.K. "Three-Parameter Model for Debonding of FRP Plate from Concrete Substrate", *ASCE Journal of Engineering Mechanics* , Vol..132, No.5, pp.509-518, 2006.

Malek, A. M., Saadatmanesh, H., and Ehsani, M. R. (1998), *Prediction of Failure Load of R/C Beams Strengthened with FRP Plate Due to Stress Concentration at Plate End*, ACI Structural Journal, Vol. 95, No. 2, pp. 142-152.

Meier U., Deuring, M., Meier, H., and Schwegler, G. (1992). "strengthening of structures with CFRP laminates: Research and applications in Switzerland." *Advanced composite materials in bridges and structures*, Canadian Society for Civil Engineering, 243-251.

Meier U. "Strengthening of structures using carbon fibre/epoxy composites", Constr Building Material; 9(6):341-351, 1995.

Meier U. Post strengthening by continuous fiber laminates in Europe. Non-metallic (FRP) reinforcement for concrete structures, vol.1. Japan Concrete Institute; 1997. p. 41–56.

Nguyen D.M., Chan T.K., and Cheong H.K. (2001). "Brittle failure and bond development length of CFRP concrete beams." *Journal of Composites for Construction*, vol. 5, no. 1, pp.12-17.

Niu and Wu "Analytical modeling on debonding failure of FRP-strengthened RC flexural structures" International Conference paper, 2002.

Oehlers, D. J. (1992), *Reinforced Concrete Beams with Plates Glued to Their Soffits*, Journal of Structural Engineering, ASCE, Vol. 118, No. 8, pp. 2023-2038.

Pan Jinlong and Christopher K.Y. Leung, (2007). "Debonding along the FRP-concrete interface under combined pulling/peeling effects", Engineering Fracture Mechanics, 74(1), 132-150.

Raoof, M. and Zhang, S. (1997), *An insight into the Structural Behaviour of Reinforced Concrete Beams with Externally Bonded Plates*, Proceedings of the Institution of Civil Engineers: Structures and Buildings, Vol. 122, November, pp. 477-492.

Raoof, M., and Hassanen, M. A. H. (2000), *Peeling Failure of Reinforced Concrete Beams with Fibre-Reinforced Plastic or Steel Plates Glued to Their Soffits*, Proceedings of the Institution of Civil Engineers, Structures and Buildings, Vol. 140, pp. 291-305.

Ritchie P.A., Thomas D.A., Lu L.W., and Connelly G.M., (1991). "External strengthening of concrete beams using fiber reinforced plastics." *ACI structural Journal*, 88, 490-500.

Saadatmanesh H., Ehsani M.R., (1991). "RC beams strengthened with GFRP plates. I: experimental study." *Journal of Structural Engineering*, 117(11), 3417-343.

Saadatmanesh H., and Malek A.M. (1998). "Design guidelines for strengthening of RC beam with FRP plates." *Journal of Composites for Construction*, vol. 2, no. 4, p.158-164.

Sharif A., Alsulaimani G.J., and Ghaleb B.N. (1994). "Strengthening of initially loaded reinforced concrete beams using FRP plates." *ACI Structural Journal*, vol. 91, no.2, p.160-168.

Smith, S. T., and Teng, J.G. (2002), *FRP-Strengthened RC Beams II: Assessment of Debonding Strength Models*, Engineering Structures, Vol. 24, No. 4, pp. 397-417.

Taljsten B. "Strengthening of concrete prisms using the plate-bonding technique", *International Journal of Fracture*, 82: 253-266, 1996.

Teng J.G., Smith S.T., Yao J., Chen J.F. 2003. Intermediate crack-induced debonding in RC beams and slabs, *Construction and Building Materials*, 17(6-7):447-462.

Wang J. 2006. Debonding of FRP-plated reinforced concrete beam, a bond-slip analysis. I. Theoretical formulation, *International Journal of Solids and Structures*, 43(21):6649-6664.

Wang J. 2007. Cohesive zone model of FRP-concrete interface debonding under mixed-mode loading, *International Journal of Solids and Structures*, 44(20):6551-6568.

Ziraba Y.N., Baluch MH, Basunbul IA, Sharif AM, Azad AK, Al-Sulaimani GJ. (1994). "Guideline towards the design of reinforced concrete beams with external plates." *ACI Structural Journal*, 91(6), pp.639-646